RESEARCH ARTICLE

WILEY

Neural mechanism and heritability of complex motor sequence and audiovisual integration: A healthy twin study

Zhi Li[1,2]* (ORCID) | Jia Huang[1,2]* (ORCID) | Ting Xu[3,4]* | Ya Wang[1,2] | Ke Li[5] |
Ya-Wei Zeng[5] | Simon S. Y. Lui[1,6] | Eric F. C. Cheung[6] | Zhen Jin[5] |
Paola Dazzan[7,8] | David C. Glahn[9] (ORCID) | Raymond C. K. Chan[1,2] (ORCID)

[1]Neuropsychology and Applied Cognitive Neuroscience Laboratory, CAS Key Laboratory of Mental Health, Institute of Psychology, Chinese Academy of Sciences, Beijing, China

[2]Department of Psychology, The University of Chinese Academy of Sciences, Beijing, China

[3]CAS Key Laboratory of Behavioral Sciences, Institute of Psychology, Chinese Academy of Sciences, Beijing, China

[4]Center for the Developing Brain, Child Mind Institute, New York, New York

[5]MRI Center, Hospital 306, Beijing, China

[6]Castle Peak Hospital, Hong Kong Special Administrative Region, Hong Kong, China

[7]Department of Psychosis Studies, Institute of Psychiatry, Psychology and Neuroscience, King's College London, London, United Kingdom

[8]National Institute for Health Research (NIHR) Biomedical Research Centre at South London and Maudsley NHS Foundation Trust and King's College London, London, United Kingdom

[9]Department of Psychiatry, Yale University & Olin Neuropsychiatric Research Center, Institute of Living, United States of America

Correspondence
Raymond C. K. Chan, 16 Lincui Road, Chaoyang District, Beijing 100101, China.
Email: rckchan@psych.ac.cn

Funding information
Beijing Municipal Science & Technology Commission Grant, Grant/Award Number: Z161100000216138; National Key Research and Development Programme, Grant/Award Number: 2016YFC0906402; Beijing Training Project for the Leading Talents in S & T, Grant/Award Number: Z151100000315020; "Strategic Priority Research Program (B)" of the Chinese Academy of Sciences, Grant/Award Number: XDB02030002; Outstanding Young Investigator Award of the National Science Fund China, Grant/Award Number: 81088001; CAS Key Laboratory of Mental Health, Institute of Psychology

Abstract

Complex motor sequencing and sensory integration are two key items in scales assessing neurological soft signs. However, the underlying neural mechanism and heritability of these two functions is not known. Using a healthy twin design, we adopted two functional brain imaging tasks focusing on fist-edge-palm (FEP) complex motor sequence and audiovisual integration (AVI). Fifty-six monozygotic twins and 56 dizygotic twins were recruited in this study. The pre- and post-central, temporal and parietal gyri, the supplementary motor area, and the cerebellum were activated during the FEP motor sequence, whereas the precentral, temporal, and fusiform gyri, the thalamus, and the caudate were activated during AVI. Activation in the supplementary motor area during FEP motor sequence and activation in the precentral gyrus and the thalamic nuclei during AVI exhibited significant heritability estimates, ranging from 0.5 to 0.62. These results suggest that activation in cortical motor areas, the thalamus and the cerebellum associated with complex motor sequencing and audiovisual integration function may be heritable.

KEYWORDS

audiovisual integration, fist-edge-palm, fMRI, healthy twin, heritability

1 | INTRODUCTION

Complex motor sequencing and sensory integration are two key items in scales assessing neurological soft signs such as the Cambridge

---

*Zhi Li, Jia Huang, and Ting Xu contributed equally to this work.

Neurological Inventory (CNI) and the Neurological Evaluation Scale (NES) (Buchanan and Heinrichs, 1989; Chen et al., 1995). Deficits in complex motor sequencing and sensory integration are prevalent in psychiatric disorders including schizophrenia, bipolar disorder, autism, and attention-deficit hyperactive disorders (Buchanan and Heinrichs, 1989; Chan and Gottesman, 2008; Chan, Xu, Heinrichs, Yu, & Wang,

2010b; Heinrichs and Buchanan, 1988; Peng et al., 2012; Zhao et al., 2013). Although many studies have focused on these impairments in psychiatric disorders, their underlying neural mechanism and whether these impairments are heritable is not known. Empirical evidence has demonstrated that the grey matter volumes of the pre- and postcentral gyri, and the frontal and temporal lobes were associated with impairments in complex motor sequencing, sensory integration, or both in healthy individuals (Dazzan et al., 2006; Hirjak, Thomann, Kubera, Stieltjes, & Wolf, 2016a; Hirjak, Wolf, Kubera, Stieltjes, & Thomann, 2016b; Thomann, Hirjak, Kubera, Stieltjes, & Wolf, 2015). While the evidence for the association between complex motor sequencing/sensory integration and subcortical volumes was found in patients with schizophrenia, similar associations have not been found in healthy controls (Bottmer et al., 2005; Dazzan et al., 2004; Heuser et al., 2011; Ho, Mola, & Andreasen, 2004; Kong, Bachmann, Thomann, Essig, & Schroder, 2012; Mouchet-Mages et al., 2007; Thomann et al., 2009; Venkatasubramanian, Jayakumar, Gangadhar, & Keshavan, 2008). It is possible that these inconsistent findings reflect the specific pathophysiology of schizophrenia, or the effect of antipsychotic medications in individuals with this disorder (Hirjak et al., 2016b; Thomann et al., 2015).

The examination of motor and sensory integratory function in healthy individuals provides an opportunity to investigate the underlying neural mechanism without the confounding effect of antipsychotic exposure. However, evidence on the brain activation changes associated with complex motor sequencing, such as the Luria's fist-edge-palm task, and sensory integration in healthy individuals remains limited. In contrast with the traditional dichotomous scoring system in the clinical assessment of complex motor sequencing and sensory integration which may be influenced by individual judgement (Sanders et al., 2006), using functional brain imaging tasks to investigate brain activation changes associated with complex motor sequencing and sensory integration can circumvent this problem. To date only two studies, both with limited sample size, have examined brain activations when performing the Luria's Fist-Edge-Palm (FEP) task, a classic task that captures complex motor sequencing. Both studies reported significant activations in the sensorimotor, premotor, and cerebellar areas during the FEP task (Chan, Rao, Chen, Ye, & Zhang, 2006; Umetsu et al., 2002). Two previous studies reported thalamic activation during the execution of audiovisual integration tasks, supporting the role of the thalamus in sensory integration (Bonath et al., 2013; Jakobs et al., 2012). However, no study has yet explored the underlying neural mechanism of FEP motor sequence and audiovisual integration simultaneously using an adequately powered sample.

Impairments in complex motor sequencing and sensory integration observed in unaffected first degree relatives of patients with schizophrenia and at-risk individuals suggests that these signs may be heritable (Chan et al., 2010a; Compton et al., 2007; Griffiths, Sigmundsson, Takei, Rowe, & Murray, 1998; Picchioni et al., 2006; Yazici, Demir, Yazici, & Gogus, 2002). However, only two studies have quantified the heritability of these deficits so far. Sanders et al. (2006) found a high heritability, ranging from 0.53 to 0.99, in patients with schizophrenia. Consistent with these findings, we recently reported significant, albeit

more moderate, heritability of complex motor function, in an independent healthy twin sample (Xu et al., 2016).

In this study, we aimed to delineate the brain circuits subserving motor and sensory integrative function in healthy individuals, using a FEP and an AVI task. In addition, we aimed to establish the heritability of this neural activation. We hypothesized that (a) the pre- and postcentral gyri and the cerebellum would be activated when performing the FEP task, while subcortical areas such as the thalamus would be activated during the AVI task, and (b) these activations would be heritable.

2 | METHODS

2.1 | Participants

Twenty-eight pairs of monozygotic twins and 28 pairs of dizygotic twins were recruited from the twin pool of the Institute of Psychology, the Chinese Academy of Sciences. Three pairs of twins were excluded due to excessive head motions during fMRI scanning, with a Frame Displacement (FD) value larger than 0.25 (Power, Barnes, Snyder, Schlaggar, & Petersen, 2012). Hence 26 pairs of monozygotic twins (12 male pairs; age = 18.5 ± 0.9; education year = 13.37 ± 0.93; IQ = 112.02 ± 16.2) and 27 pairs of dizygotic twins (13 male pairs; age = 19.63 ± 1.61; education year = 13.2 ± 1.56; IQ = 111.11 ± 14.04) were included in the final analysis. The exclusion criteria were a history of craniocerebral trauma, cerebral organic disease, substance abuse, diagnosed mental disorder, left-handedness, and having first-degree relatives with a diagnosed mental disorder. The short form of the Chinese version of the Wechsler Adult Intelligence Scale-Revised (WAIS-R) (Gong, 1992) was administered to all participants to exclude those with an intelligence quotient (IQ) lower than 70. This study was approved by the Ethics Committee of the Institute of Psychology, the Chinese Academy of Sciences. All participants gave written informed consents.

2.2 | The fist-edge-palm (FEP) task

The applicability and reliability of the FEP task has been described elsewhere (Chan et al., 2006). This study adopted a short version of the FEP task which consisted of the FEP motor sequence and palm-tapping (PT) (control task). All participants were asked to perform the FEP and the PT motor sequences alternately according to demonstration pictures displayed on a screen in the MRI scanner. In each block, a 20-s fixed cross and a 6-s signature indicated whether the FEP or the PT task should be executed followed by the demonstration picture. The FEP block contained three pictures demonstrating the fist, the edge and the palm in turn which lasted for 40.5 s, while the PT block contained two pictures demonstrating the palm-tapping and the palm-lifting actions which lasted for 40 s. Two 7-min runs of tasks each containing three blocks of FEP motor sequence and three blocks of PT motor sequence were administered. The order of the blocks was counterbalanced among the participants (Figure 1).
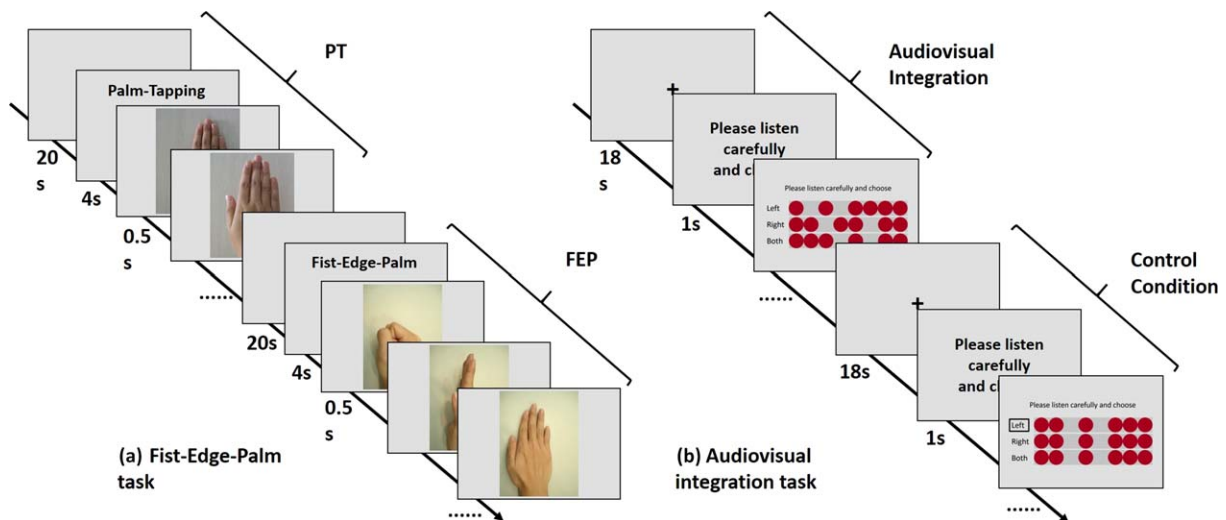
FIGURE 1 Workflow of the fist-edge-palm and audiovisual tasks: (a) The fist-edge-palm task. (b) The audiovisual integration task

2.3 | The audiovisual integration (AVI) task

The AVI task designed by our laboratory contains both audiovisual integration and control conditions (Huang et al., 2012). In the audiovisual integration condition, participants were asked to choose a matching dotted line with the tone sequence from a three-line dot matrix. Participants were told to press the left button to choose the first line, right button for the second line, and both buttons for the third line. In the control condition, participants were required to choose the dotted line with a black square in front regardless of the tone sequence. The Morse tone sequence consisted of 350 ms pure tones and blank tones with a 200-ms interval between the two tones. Five blocks with eight trials of audiovisual integration and five blocks with eight trials of control conditions were alternately presented to the participants (Figure 1). The whole AVI task lasted 7 min and 46 s.

2.4 | MRI data acquisition

All the imaging data were collected in a 3-T scanner system (MAGNE-TOM® Verio Siemens). Two radiologists ruled out any obvious neurological abnormalities based on a T2-weighted image (TR = 4,000 ms; TE = 90 ms; FOV = 200 mm; slices = 19; flip angle = 120 degree; image matrix = 256 × 512; voxel dimensions = 0.9 mm × 0.4 mm × 5 mm). Then a high-resolution structural brain image was acquired with the sequence: TR = 2300 ms; TE = 3 ms; FOV = 256 mm; flip angle = 9°; image matrix = 256 × 256; voxel dimensions = 1 mm × 1 mm ×1 mm. Finally, an echo planner imaging sequence (TR = 2000 ms; TE = 30 ms; FOV = 210 cm; slices = 32; flip angle = 90°; image matrix = 64 × 64; voxel dimensions = 3.3 mm ×3.3 mm ×4 mm) was adopted to acquire the brain functional imaging data. Head movement was controlled by a head-holding pad.

2.5 | MRI data analysis

The Statistical Parametric Mapping 8 (SPM8, http://www.fil.ion.ucl.ac.uk/spm/) was used to analyze the functional imaging data. The raw images were first corrected in time and space, followed by registration to the individual high-resolution structural image with DARTEL (Ashburner, 2007). We ruled out the effect of head motion through excluding twins with a mean FD larger than 0.25 (Power et al., 2012), and including the six head movement parameters in the general linear model (GLM), similar to traditional task-based fMRI studies (SPM8, http://www.fil.ion.ucl.ac.uk/spm/). All the images were nonlinearly normalized to the brain template of the Montreal Neurological Institute (MNI) and smoothed with an 8-mm full-width at half-maximum Gaussian kernel.

The FEP and PT motor sequences of the FEP task, and the AVI and control conditions of the AVI task were included into two GLM with SPM8, with the six head movement parameters of each task as covariates to control for motion effects. One sample t tests were used to examine whole brain activation during the FEP and PT motor sequences, the AVI and control conditions, and their respective contrasts. Given the strong brain activation of the present block study design, we adopted a stringent statistic threshold to identify the peak point of each cluster. The threshold for the whole brain analysis was set at $p < .0001$ with familiar-wise-error (FWE) correction at the voxel level with the cluster size larger than 100. Finally, the average t-contrast value of a 6-mm-radius sphere centered at each peak point of each condition was extracted from the t-contrast file generated from the GLM to calculate heritability. Gender, age, and IQ were regressed out from the extracted t value.

2.6 | Quantitative genetic analyses

Using the structure equation modeling tool OpenMx (http://openmx.psyc.virginia.edu/), the variance and covariance of each phenotype (the average t contrast value extracted from 6-mm-radius spheres centered at each peak point of brain activation during task performance) were parsed into three sources: additive genetic component (A), common environmental component (C), and unique environmental component (E). Based on the a-priori assumption in behavioural genetics,

monozygotic twins share (nearly) 100% of their segregating genes, whereas dizygotic twins share, on average, 50%. The full univariate ACE model which contained all the A, E, and C factors, was compared with its nest submodels AE and CE. Similarly, model E was compared with model AE and CE, respectively. The model with the smallest Akaike Information Criterion (AIC) was chosen as the optimal model (please refer to Supporting Information for details on model selection). Statistical inference was carried out by comparing the likelihood ratio chi-squared statistic and minus two times log likelihood difference ($-2LL$) of the models. The heritability estimate of the brain activation was considered significant if the AE model was the optimal model which significantly deteriorated if factor A was removed and if the 95% confidence interval of the standardized heritability estimate did not contain zero. Heritability was estimated based on the proportion of additive genetic component in explaining the variance (details of the statistical values of the ACE, AE, CE, and E models of each region of interest can be found in the Supporting Information) (Kim, 2010; Neale and Maes, 2004). Multiple testing of genetic model comparisons in each contrast was adjusted with Bonferroni correction. We also examined the heritability of the FD value of the FEP and AVI tasks. The E model was chosen as the optimal model for the FD values of both tasks, as it denoted the head movement patterns were not heritable in this study.

3 | RESULTS

3.1 | Brain activation and heritability of the fist-edge-palm motor sequence task

The bilateral precentral gyrus, the left postcentral gyrus, the left supplementary motor area, the bilateral insula, the bilateral inferior frontal gyrus, the right inferior temporal, the left middle temporal gyri, the right cerebellar cuneus, and the lingual gyrus were activated when participants performed the PT motor sequence, whereas the bilateral precentral gyrus, the left postcentral gyrus, the left supplementary motor area, the bilateral middle temporal gyrus, the right insula, the left inferior parietal lobule, and the cerebellar culmen were activated when participants performed the FEP motor sequence. Compared with the PT motor sequence, the FEP motor sequence activated the bilateral precentral gyrus, the left postcentral gyrus, the left superior parietal lobule, and the right cerebellar culmen more (Table 1 and Figure 2a).

Activation in the left postcentral gyrus (h^2 (95%CI) = 0.75 (0.57,0.86), $p < .001$) and the left insula (h^2 (95%CI) = 0.42(0.12,0.64), $p = .032$) associated with the PT motor sequence, and activation in the left supplementary motor area (h^2 (95%CI) = 0.5(0.19,0.72), $p = .015$) associated with the FEP sequence showed significant heritability (Table 1).

3.2 | Brain activation and heritability of the audiovisual integration task

The right transverse temporal gyrus, the superior temporal gyrus, the inferior frontal gyrus, the medial frontal gyrus, the inferior parietal lobule, the superior parietal lobule, the left precuneus, the fusiform gyrus, the lingual gyrus, and the cerebellar declive were activated during the control condition of the audiovisual integration (AVI) task, whereas the bilateral precentral gyrus, the right superior temporal gyrus, the right claustrum, the right precuneus, the fusiform gyrus, the bilateral thalamus, and the bilateral caudate were activated during the AVI condition. Compared with the control condition, the AVI condition was associated with more activation in the bilateral precentral gyrus, the bilateral precuneus, the left superior parietal lobule, and the bilateral thalamus (Table 2 and Figure 2b).

Activation in the left medial frontal gyrus (h^2 (95%CI) = 0.51 (0.36,0.7), $p < .001$), right fusiform gyrus (h^2 (95%CI) = 0.57(0.26,0.76), $p = .01$), the left lingual gyrus (h^2(95%CI) = 0.68(0.45,0.82), $p < .001$), and the left inferior parietal lobule (h^2(95%CI) = 0.49(0.36,0.71), $p = .04$) associated with the control condition, and activation in the right precentral gyrus (h^2(95%CI) = 0.62(0.36,0.78), $p < .001$) and the right thalamic ventral lateral nucleus (h^2(95%CI) = 0.58(0.28,0.76), $p < .001$) exhibited significant heritability. However, only the heritability estimate of the activation in the right subgyral (h^2(95%CI) = 0.64 (0.4,0.8), $p < .001$) associated with the contrast "AVI versus control" was significant (Table 2).

4 | DISCUSSION

Consistent with our hypothesis, the pre- and postcentral, the middle temporal, inferior and parietal gyri, the supplementary motor area, the insula, and the cerebellar culmen were significantly activated when healthy participants performed the FEP motor sequence. The precentral, superior temporal and fusiform gyri, the thalamus, the caudate, and the cerebellar declive were significantly activated with audiovisual integration (AVI). We also found activation in the pre- and postcentral gyri, the superior parietal gyri, and the cerebellar culmen in the contrast "FEP versus PT," and activation in the precentral gyrus, precuneus, and thalamus in the contrast "AVI versus control." Furthermore, brain activation in the supplementary motor area during FEP motor sequence performance and activation in the precentral gyrus and the thalamic nuclei during audiovisual integration also exhibited significant heritability.

Two previous studies which examined the neural mechanism of the FEP task in healthy people found that the sensorimotor cortex, the premotor cortex, the supplementary motor area, the parietal gyrus, and the cerebellum were engaged with this complex motor sequence (Chan et al., 2006; Umetsu et al., 2002). In our study, activation of the pre- and postcentral gyrus, the supplementary motor area, the inferior parietal gyrus, and the cerebellar culmen during the FEP motor sequence was consistent with these previous findings. Motor areas have been suggested to be sensitive to the complexity of motor sequences such that more difficult tasks may be associated with greater activation in these areas (Catalan, Honda, Weeks, Cohen, & Hallett, 1998; Kawashima et al., 1998). The parietal gyrus plays a role in monitoring hand movement through the integration of visual information (Clower et al., 1996; Kertzman, Schwarz, Zeffiro, & Hallett, 1997). Finally, the

TABLE 1 Brain activation and corresponding heritability of the fist-edge-palm task and the palm-tapping task

Region (L/R)	VS (T)	Peak coord.	Optimal model	p^a	p^b	h^2 (95% CI)	c^2 (95% CI)	e^2 (95% CI)
PT								
Precentral gyrus (L)	298(11.33)	[−48,0,3]	AE	.148	.592	0.24 (0,0.53)	\	0.76 (0.47,1)
Postcentral gyrus (L)	2555(26.34)	[−27,−27,57]	AE	<.001**	<.001**	0.75 (0.57,0.86)	\	0.25 (0.14,0.43)
Insula (L)	2555(18.23)a	[−45,−27,21]	AE	.008**	.032*	0.42 (0.12,0.64)	\	0.58 (0.36,0.88)
Supplementary motor area (L)	2555(17.56)a	[−6,−18,51]	AE	.063	.252	0.32 (0,0.59)	\	0.68 (0.41,1)
Cerebellar cuneus (R)	739(7.69)a	[18,−99,3]	E	\	\	\	\	1(1,1)
Inferior temporal gyrus (R)	739(19.83)	[48,−66,0]	E	\	\	\	\	1(1,1)
Insula (R)	545(13.25)	[57,−27,21]	E	\	\	\	\	1(1,1)
Cerebellar lingual (R)	444(18.54)	[9,−51,−15]	E	\	\	\	\	1(1,1)
Inferior frontal gyrus (R)	436(8.02)a	[63,9,21]	E	\	\	\	\	1(1,1)
Precentral gyrus (R)	436(10.18)	[54,3,45]	E	\	\	\	\	1(1,1)
Inferior frontal gyrus (L)	298(7.81)a	[−39,24,−15]	E	\	\	\	\	1(1,1)
Middle temporal gyrus (L)	281(15.49)	[−48,−66,6]	E	\	\	\	\	1 (1,1)
FEP								
Supplementary motor area (L)	2600(19.74)b	[−6,−3,57]	AE	.003**	.015*	0.5 (0.19,0.72)	\	0.5 (0.28,0.81)
Postcentral gyrus (L)	2600(29.72)	[−36,−24,54]	CE	<.001**	<.001**	\	0.64 (0.45,0.77)	0.36 (0.23,0.55)
Middle temporal gyrus (R)	1236(19.53)	[51,−66,0]	CE	<.001**	<.001**	\	0.46 (0.23,0.65)	0.54 (0.35,0.77)
Cerebellar culmen (R)	1236(19.32)a	[6,−60,−21]	CE	.149	.745	\	0.2 (0,0.44)	0.8 (0.56,1)
Middle temporal gyrus (L)	190(13.3)	[−48,−66,3]	CE	.017*	.085	\	0.32 (0.06,0.54)	0.68 (0.46,0.94)
Inferior parietal lobule (R)	153(9.58)	[39,−39,51]	E	\	\	\	\	1 (1,1)
Precentral gyrus (L)	151(11.71)	[57,6,42]	E	\	\	\	\	1 (1,1)
Precentral gyrus (R)	151(9.3)a	[60,9,30]	E	\	\	\	\	1 (1,1)
Insula (R)	127(8.66)	[57,−27,21]	E	\	\	\	\	1 (1,1)
FEP vs PT								
Postcentral gyrus (L)	1160(15.57)	[−39,−21,57]	AE	.055†	.11	0.31 (0,0.57)	\	0.69 (0.43,1)
Precentral gyrus (L)	1160(13.47)a	[−27,−12,63]	AE	.135	.27	0.25 (0,0.54)	\	0.75 (0.46,1)
Superior parietal lobule (L)	1160(10.44)a	[−30,−54,63]	E	\	\	\	\	1 (1,1)
Precentral gyrus (R)	194(11.76)	[33,−12,66]	E	\	\	\	\	1 (1,1)
Cerebellar culmen (R)	103(9.29)	[21,−51,−24]	E	\	\	\	\	1(1,1)

Note. Abbreviations: Coord. = Coordinate; c^2 = common environment effect; e^2 = random environment effect; CI = confidence interval; FEP = fist-edge-palm; PT = palm-tapping; a, part of cluster above; R = right; L = left; h^2 = heritability/additive genetic effect; VS(T) = voxel size (T value).

[a]Uncorrected p.

[b]Bonferroni adjusted-p.

*p < .05; **p < .01; the p value listed here indicated the deterioration after abandoning the factor A. Statistical threshold of whole brain activation was set as p < .0001 with familiar-wise-error (FWE) correction at voxel level, cluster size > 100.
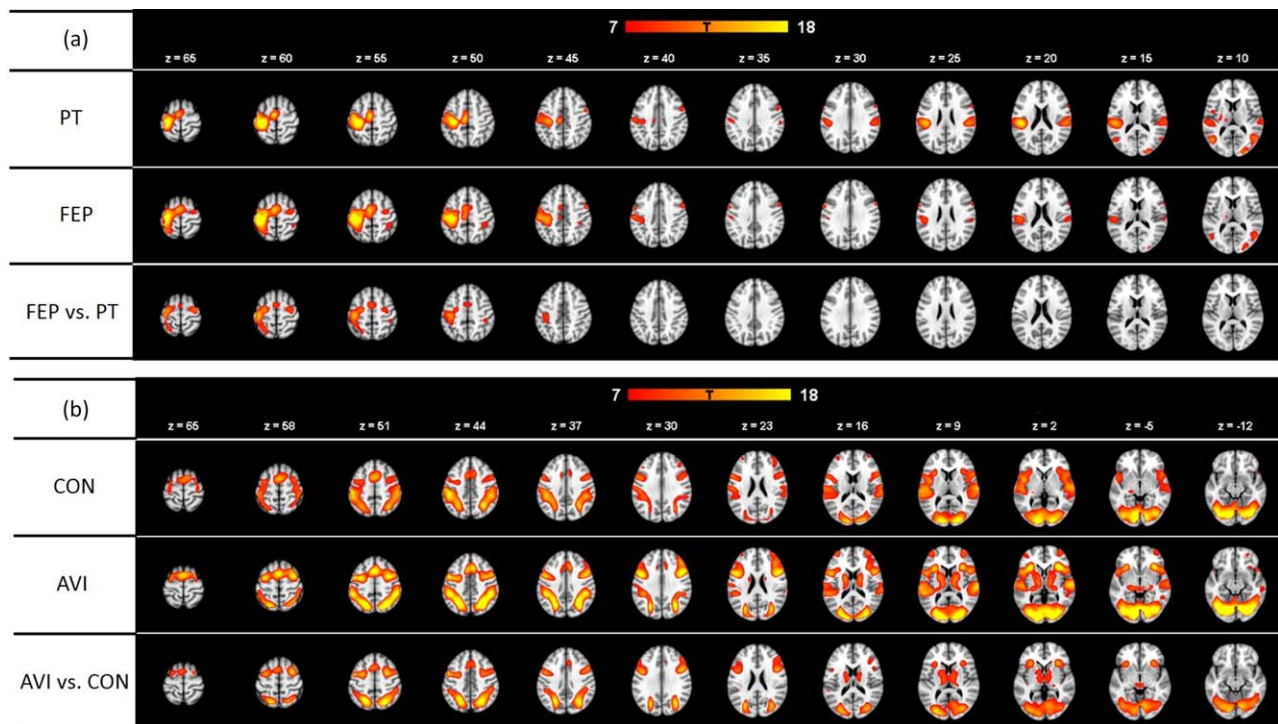
FIGURE 2 Whole-brain activation of the fist-edge-palm and audiovisual tasks: (a) The fist-edge-palm task, each row showing the whole activation in palm-tapping (PT), fist-edge-palm (FEP), and FEP vs PT, respectively. (b) The audiovisual integration task, each row showing the whole activation in control condition (CON), audiovisual integration (AVI), and AVI vs CON, respectively. The red–orange color bar indicates the strength of activation (*T* value). The *z* value indicates the transect coordinates in the Montreal Neurological Institute (MNI) atlas

cerebellum has been considered essential in motor learning and coordination (Imamizu et al., 2000). In contrast to the simple PT motor sequence, the FEP task was associated with more activation in the pre- and postcentral gyrus and the cerebellum, which corroborated with these suggestions. In this study, we also found increased activation at the middle temporal gyrus, which have not been reported in the two previous functional imaging studies. However, previous morphometric correlation studies have reported significant associations between complex motor sequencing and grey matter volumes of the insula and the temporal gyrus, which to some extent supported our findings (Heuser et al., 2011; Venkatasubramanian et al., 2008). The insula and the extended claustrum have been suggested to play a role in integrating information across sensory modalities (Augustine, 1996; Calvert, 2001). Activation of the prefrontal gyrus, which has been conventionally viewed as the core brain region associated with FEP performance (Luria, 1966), was not observed in both the present and the previous two studies. It is possible that the prefrontal gyrus plays only a regulatory role in complex motor sequences, and the traditional general linear model on blood level oxygen dependency signals may not be sensitive enough to detect any change (Rao, Di, Chan, Ding, Ye, & Gao, 2008).

We also found that the precentral, the superior temporal, the fusiform gyri, the thalamus, the caudate and the cerebellar declive were activated during the AVI task. Activation of the temporal and the fusiform gyri may reflect audio and visual information processing and integration (Dazzan et al., 2004). Activation of the thalamus appears to be specific to AVI, as it was not observed in the control condition in which

audiovisual information was not integrated. In addition, activation of various nuclei of the thalamus was also identified in the contrast AVI vs control condition, which supported a role for the thalamus in sensory integration. These findings are consistent with previous studies which also reported activation of the thalamus when performing AVI (Bonath et al., 2013; Jakobs et al., 2012). Consistent with our results, evidence from both animal and human data supports the relay role of the thalamus in multiple sensory integration (Allen, Procyk, Brown, & Lucas, 2017; Stafford and Huberman, 2017).

Activation of the pre- and postcentral gyri, the temporal gyrus, the insula and the cerebellar areas during the FEP motor sequence, and activation of the precentral, superior temporal and fusiform gyri during audiovisual integration were consistent with evidence from previous structural MRI studies of complex motor sequencing in healthy individuals (Dazzan et al., 2006; Hirjak et al., 2016a,b; Thomann et al., 2015). These findings suggest that the FEP and AVI tasks can capture the complex motor sequencing and sensory integration functions. However, previous sMRI studies failed to find any correlation between sensory integration and subcortical volumes. Several points should be kept in mind in interpreting these inconsistencies. First, in contrast to previous studies on brain morphology of healthy individuals, we directly measured brain activation during a sensory integration task. Second, the dichotomous scoring system of traditional behavioral assessments of sensory integration may not be able to fully delineate the relevant subtle expression in healthy individuals. Therefore, studies examining the structural correlates of sensory integration measured by behavioral

TABLE 2 Brain activation and corresponding heritability of the audiovisual integration task and the control task

Region (L/R)	VS (Z)	Peak coord.	Optimal model	p^a	p^b	h^2 (95%CI)	c^2 (95%CI)	e^2 (95%CI)
CON								
Transverse temporal gyrus (R)	930 (15.51)	[66,−19,7]	AE	0.015*	0.05*	0.41 (0.09,0.65)	/	0.59 (0.35,0.91)
Superior temporal gyrus (R)	930 (12.58)a	[57,−34,13]	AE	0.112	1	0.27 (0,0.56)	/	0.73 (0.44,1)
Inferior frontal gyrus (R)	930 (12.28)a	[57,14,13]	AE	0.087	0.87	0.27 (0,0.54)	/	0.73 (0.46,1)
Medial frontal gyrus (L)	396 (15.87)	[0,5,55]	AE	<0.001**	<0.001**	0.51 (0.36,0.7)	/	0.49 (0.3,0.64)
Cerebellar declive (L)	3921 (22.51)	[−39,−76,−14]	AE	0.133	1	0.29 (0,0.59)	/	0.71 (0.41,1)
Fusiform gyrus (R)	3921 (21.95)a	[36,−76,−11]	AE	0.001**	0.01*	0.57 (0.26,0.76)	/	0.43 (0.24,0.74)
Lingual gyrus (L)	3921 (21.45)a	[−9,−82,−5]	AE	<0.001**	<0.001**	0.68 (0.45,0.82)	/	0.32 (0.18,0.55)
Inferior parietal lobule (L)	2147 (18.56)	[−48,−31,46]	AE	0.004**	0.04*	0.49 (0.36,0.71)	/	0.51 (0.29,0.64)
Superior parietal lobule (R)	944 (18.53)	[30,−58,46]	CE	0.035*	0.35	/	0.28 (0.02,0.51)	0.72 (0.49,0.98)
Inferior parietal lobule (R)	944 (15.39)a	[51,−31,52]	CE	0.014*	0.14	/	0.33 (0.07,0.54)	0.67 (0.46,0.93)
Precuneus (L)	2147 (15.92)	[−27,−61,46]	E	/	/	/	/	1 (1,1)
AVI								
Cerebellar declive (L)	7966 (27.42)	[−12,−82,−14]	AE	0.08	0.8	0.31 (0,0.58)	/	0.69 (0.42,1)
Precentral gyrus (R)	3672 (23.32)	[45,8,31]	AE	<0.001**	<0.001**	0.62 (0.36,0.78)	/	0.38 (0.22,0.64)
Claustrum (R)	3672 (21.8)a	[33,23,4]	AE	0.016*	0.16	0.45 (0.21,0.69)	/	0.55 (0.31,0.79)
Thalamus (ventral lateral nucleus) (L)	317 (12.5)	[−15,−7,4]	AE	0.008**	0.08	0.5 (0.14,0.73)	/	0.5 (0.27,0.86)
Thalamus (L)	317 (12.41)a	[−12,−16,7]	AE	0.041*	0.41	0.42 (0.02,0.69)	/	0.58 (0.31,0.98)
Thalamus (medial dorsal nucleus) (R)	286 (12.42)	[12,−16,7]	AE	0.012*	0.12	0.5 (0.12,0.74)	/	0.5 (0.26,0.8)
Thalamus (ventral lateral nucleus) (R)	286 (12.41)a	[15,−7,10]	AE	<0.001**	<0.001**	0.58 (0.28,0.76)	/	0.42 (0.24,0.72)
Precuneus (R)	7966 (25.71)a	[24,−64,49]	CE	<0.001**	<0.001**	/	0.51 (0.28,0.68)	0.49 (0.32,0.72)
Caudate body (L)	317 (14.13)	[−18,−4,16]	CE	0.002313	0.002313	/	0.4 (0.15,0.6)	0.6 (0.4,0.85)

(Continues)

TABLE 2 (Continued)

Region (L/R)	VS (Z)	Peak coord.	Optimal model	p^a	p^b	h^2 (95%CI)	c^2 (95%CI)	e^2 (95%CI)
Caudate body (R)	286 (12.33)a	[18,−4,19]	CE	0.004149	0.004149	✓	0.38 (0.13,0.58)	0.62 (0.42,0.87)
Fusiform gyrus (L)	7966 (26.01)	[−33,−79,−11]	E	✓	✓	✓	✓	1 (1,1)
Superior temporal gyrus (R)	402 (17.83)	[63,−22,7]	E	✓	✓	✓	✓	1 (1,1)
Precentral gyrus (L)	3672 (22.58)a	[−48,5,31]	E	✓	✓	✓	✓	1 (1,1)
AVI vs CON								
Precentral gyrus (L)	3204 (17.31)	[−48,−1,49]	AE	0.015*	0.105	0.44 (0.09,0.68)	✓	0.56 (0.32,0.91)
Subgyral (R)	3204 (17.04)a	[30,2,58]	AE	<0.001**	<0.001**	0.65 (0.4,0.8)	✓	0.35 (0.2,0.6)
Precuneus (R)	7162 (21.23)	[24,−64,46]	CE	0.056988	0.056988	✓	0.26 (0,0.49)	0.74 (0.51,1)
Superior parietal lobule (L)	7162 (20.72)a	[−21,−61,52]	CE	0.017204	0.017204	✓	0.32 (0.06,0.54)	0.68 (0.46,0.94)
Precuneus (L)	7162 (20.2)	[−24,−64,43]	CE	0.004674	0.004674	✓	0.37 (0.25,0.58)	0.63 (0.42,0.73)
Precentral gyrus (R)	3204 (16.62)	[48,11,31]	CE	0.021082	0.021082	✓	0.31 (0.05,0.53)	0.69 (0.47,0.95)
Thalamus (ventral anterior nucleus) (L)	1030 (10.12)b	[−15,−1,10]	CE	0.152794	0.152794	✓	0.19 (0,0.44)	0.81 (0.56,1)
Thalamus (ventral lateral nucleus) (L)	1030 (10.8)	[−12,−13,10]	E	✓	✓	✓	✓	1 (1,1)
Thalamus (anterior nucleus) (R)	1030 (10.64)a	[12,−10,13]	E	✓	✓	✓	✓	1 (1,1)

Note. Abbreviations: AVI = audiovisual integration; c^2 = common environment effect; CI = confidence interval; CON = control condition; a, part of cluster above; b, part of cluster below; Coord. = Coordinate; e^2 = random environment effect; h^2 = heritability/additive genetic effect; L = Left; R = Right; VS(T) = voxel size (T value).
aUncorrected p.
bBonferroni adjusted-p.
**p < .01, the p value listed here indicated the deterioration after abandoning the factor A. Statistical threshold of whole brain activation was set as p < .0001 with familiar-wise-error (FWE) correction at voxel level, cluster size > 100.

assessments may not be sensitive enough to capture the role of the thalamus in sensory integration in healthy people. The thalamus plays an integrative role in connecting the cerebellum and cortical areas in cortical–subcortical–cerebellar circuitry. However, two previous studies in healthy individuals did not find thalamic activation during audiovisual integration (Adhikari, Goshorn, Lamichhane, & Dhamala, 2013; van Atteveldt, Formisano, Goebel, & Blomert, 2007). The inconsistency of findings in studies on AVI may be due to the use of different paradigms, and this possibility should be further explored using a meta-analytic approach.

Activation of the left supplementary motor area during the FEP motor sequence showed moderate but significant heritability ($h^2 = 0.5$). Activation of the postcentral gyrus and the insula during the PT motor sequence also showed significant heritability. Activation of the ventral lateral nucleus of the thalamus during AVI was associated with moderate heritability ($h^2 = 0.58$). These results are consistent with results from our previous study in which motor coordination (which contains the FEP task) ($h^2 = 0.57$) and sensory integration ($h^2 = 0.21$) showed significant heritability (Xu et al., 2016). Although the heritability estimated here was around 0.5, which was lower than that reported by Sanders et al. (2006), it is important to note that they adopted a family design which was different from the twin design of this study. Our findings suggest that the neural mechanisms underlying complex motor sequencing and sensory integration are influenced by genetic factors, at least to a moderate extent.

The main limitation of this study is that we did not record the behavioral performance of participants. The combination of motion capture technology with imaging in future studies may help to address this issue. Furthermore, it should be noted that although our sample size was reasonable for task-based fMRI studies, future studies should recruit a larger sample of healthy twins and extend the investigation to clinical twin samples for a more accurate heritability estimate. More sophisticated heritability estimation and correction methods, such as voxel-by-voxel brain mapping on heritability, may also be considered in future studies.

In conclusion, we found that the pre- and postcentral gyrus, the supplementary motor area, the temporal and parietal gyri, and the cerebellum were significantly activated during the FEP task. During AVI, the precentral, temporal and fusiform gyri, the thalamus, the caudate, and the cerebellum were significantly activated. The FEP and the AVI tasks appeared to be appropriate tools to examine the function of cortical–subcortical–cerebellar circuitry. Furthermore, the considerable heritability of activation at the supplementary motor area, the precentral gyrus, and the various nuclei of the thalamus supports the notion that complex motor sequencing and sensory integration are heritable from a brain-activation perspective.

ACKNOWLEDGMENTS

CONFLICTS OF INTEREST

None declared.

ORCID

Zhi Li http://orcid.org/0000-0003-4436-0916
David C. Glahn http://orcid.org/0000-0002-4749-6977
Raymond C. K. Chan http://orcid.org/0000-0002-3414-450X
Jia Huang http://orcid.org/0000-0001-7269-6797

REFERENCES

Adhikari, B. M., Goshorn, E. S., Lamichhane, B., & Dhamala, M. (2013). Temporal-order judgment of audiovisual events involves network activity between parietal and prefrontal cortices. Brain Connect, 3, 536–545.

Allen, A. E., Procyk, C. A., Brown, T. M., & Lucas, R. J. (2017). Convergence of visual and whisker responses in the primary somatosensory thalamus (ventral posterior medial region) of the mouse. The Journal of Physiology, 595, 865–881.

Ashburner, J. (2007). A fast diffeomorphic image registration algorithm. NeuroImage, 38, 95–113.

Augustine, J. R. (1996). Circuitry and functional aspects of the insular lobe in primates including humans. Brain Research. Brain Research Reviews, 22, 229–244.

Bonath, B., Tyll, S., Budinger, E., Krauel, K., Hopf, J. M., & Noesselt, T. (2013). Task-demands and audio-visual stimulus configurations modulate neural activity in the human thalamus. NeuroImage, 66, 110–118.

Bottmer, C., Bachmann, S., Pantel, J., Essig, M., Amann, M., Schad, L. R., . . . Schroder, J. (2005). Reduced cerebellar volume and neurological soft signs in first-episode schizophrenia. Psychiatry Research-Neuroimaging, 140, 239–250.

Buchanan, R. W., & Heinrichs, D. W. (1989). The Neurological Evaluation Scale (NES): A structured instrument for the assessment of neurological signs in schizophrenia. Psychiatry Research, 27, 335–350.

Calvert, G. A. (2001). Crossmodal processing in the human brain: Insights from functional neuroimaging studies. Cerebral Cortex, 11, 1110–1123.

Catalan, M. J., Honda, M., Weeks, R. A., Cohen, L. G., & Hallett, M. (1998). The functional neuroanatomy of simple and complex sequential finger movements: A PET study. Brain, 121, 253–264.

Chen, E. Y. H., Shapleske, J., Luque, R., Mckenna, P. J., Hodges, J. R., Calloway, S. P., . . . Berrios, G. E. (1995). The Cambridge Neurological Inventory - A clinical instrument for assessment of soft neurological signs in psychiatric-patients. Psychiatry Research, 56, 183–204.

Chan, R. C., & Gottesman, I. I. (2008). Neurological soft signs as candidate endophenotypes for schizophrenia: A shooting star or a Northern star? Neuroscience and Biobehavioral Reviews, 32, 957–971.

Chan, R. C., Rao, H., Chen, E. E., Ye, B., & Zhang, C. (2006). The neural basis of motor sequencing: An fMRI study of healthy subjects. *Neuroscience Letters*, *398*, 189–194.

Chan, R. C., Wang, Y., Zhao, Q., Yan, C., Xu, T., Gong, Q. Y., & Manschreck, T. C. (2010a). Neurological soft signs in individuals with schizotypal personality features. *The Australian and New Zealand Journal of Psychiatry*, *44*, 800–804.

Chan, R. C., Xu, T., Heinrichs, R. W., Yu, Y., & Wang, Y. (2010b). Neurological soft signs in schizophrenia: A meta-analysis. *Schizophrenia Bulletin*, *36*, 1089–1104.

Clower, D. M., Hoffman, J. M., Votaw, J. R., Faber, T. L., Woods, R. P., & Alexander, G. E. (1996). Role of posterior parietal cortex in the recalibration of visually guided reaching. *Nature*, *383*, 618–621.

Compton, M. T., Bollini, A. M., Mack, L. M., Kryda, A. D., Rutland, J., Weiss, P. S., ... Walker, E. F. (2007). Neurological soft signs and minor physical anomalies in patients with schizophrenia and related disorders, their first-degree biological relatives, and non-psychiatric controls. *Schizophrenia Research*, *94*, 64–73.

Dazzan, P., Morgan, K. D., Orr, K. G., Hutchinson, G., Chitnis, X., Suckling, J., ... Murray, R. M. (2004). The structural brain correlates of neurological soft signs in AESOP first-episode psychoses study. *Brain*, *127*, 143–153.

Dazzan, P., Morgan, K. D., Chitnis, X., Suckling, J., Morgan, C., Fearon, P., ... Murray, R. M. (2006). The structural brain correlates of neurological soft signs in healthy individuals. *Cerebral Cortex*, *16*, 1225–1231.

Gong, Y. X. (1992). *Manual of Wechsler Adult Intelligence Scale-Chinese version*. Changsha, China: Chinese Map Press.

Griffiths, T. D., Sigmundsson, T., Takei, N., Rowe, D., & Murray, R. M. (1998). Neurological abnormalities in familial and sporadic schizophrenia. *Brain*, *121*(Pt 2), 191–203.

Heinrichs, D. W., & Buchanan, R. W. (1988). Significance and meaning of neurological signs in schizophrenia. *The American Journal of Psychiatry*, *145*, 11–18.

Heuser, M., Thomann, P. A., Essig, M., Bachmann, S., Schroder, J. (2011). Neurological signs and morphological cerebral changes in schizophrenia: An analysis of NSS subscales in patients with first episode psychosis. *Psychiatry Research-Neuroimaging*, *192*, 69–76.

Hirjak, D., Thomann, P. A., Kubera, K. M., Stieltjes, B., & Wolf, R. C. (2016a). Cerebellar contributions to neurological soft signs in healthy young adults. *European Archives of Psychiatry and Clinical Neuroscience*, *266*, 35–41.

Hirjak, D., Wolf, R. C., Kubera, K. M., Stieltjes, B., & Thomann, P. A. (2016b). Multiparametric mapping of neurological soft signs in healthy adults. *Brain Structure &Amp; Function*, *221*, 1209–1221.

Ho, B. C., Mola, C., & Andreasen, N. C. (2004). Cerebellar dysfunction in neuroleptic naive schizophrenia patients: Clinical, cognitive, and neuroanatomic correlates of cerebellar neurologic signs. *Biological Psychiatry*, *55*, 1146–1153.

Huang, J., Wang, Y., Xu, T., Jin, Z., Handley, R., Dazzan, P., & Chan, R. C. (2012). Occipital-parietal conjunction is sensitive to the audiovisual sensory integration. The 18th Annual Meeting of the Organization for Human Brain Mapping. Beijing, China.

Imamizu, H., Miyauchi, S., Tamada, T., Sasaki, Y., Takino, R., Putz, B., ... Kawato, M. (2000). Human cerebellar activity reflecting an acquired internal model of a new tool. *Nature*, *403*, 192–195.

Jakobs, O., Langner, R., Caspers, S., Roski, C., Cieslik, E. C., Zilles, K., ... Eickhoff, S. B. (2012). Across-study and within-subject functional connectivity of a right temporo-parietal junction subregion involved in stimulus-context integration. *NeuroImage*, *60*, 2389–2398.

Kawashima, R., Matsumura, M., Sadato, N., Naito, E., Waki, A., Nakamura, S., ... Yonekura, Y. (1998). Regional cerebral blood flow changes in human brain related to ipsilateral and contralateral complex hand movements - a PET-study. *European Journal of Neuroscience*, *10*, 2254–2260.

Kertzman, C., Schwarz, U., Zeffiro, T. A., & Hallett, M. (1997). The role of posterior parietal cortex in visually guided reaching movements in humans. *Experimental Brain Research*, *114*, 170–183.

Kim, Y.-K. (2010). *Handbook of behavior genetics*. Springer.

Kong, L., Bachmann, S., Thomann, P. A., Essig, M., & Schroder, J. (2012). Neurological soft signs and gray matter changes: A longitudinal analysis in first-episode schizophrenia. *Schizophrenia Research*, *134*, 27–32.

Luria, A. R. (1966). *Higher cortical functions in man*. New York: Basic Books.

Mouchet-Mages, S., Canceil, O., Willard, D., Krebs, M. O., Cachia, A., Martinot, J. L., ... Meder, J. F. (2007). Sensory dysfunction is correlated to cerebellar volume reduction in early schizophrenia. *Schizophrenia Research*, *91*, 266–269.

Neale, M. C., & Maes, H. H. M. (2004). *Methodology for genetic studies of twins and families*. Dordrecht, The Netherlands: Kluwer Academic Publishers B.V.

Peng, Z., Lui, S. S., Cheung, E. F., Jin, Z., Miao, G., Jing, J., & Chan, R. C. (2012). Brain structural abnormalities in obsessive-compulsive disorder: Converging evidence from white matter and grey matter. *Asian Journal of Psychiatry*, *5*, 290–296.

Picchioni, M. M., Toulopoulou, T., Landau, S., Davies, N., Ribchester, T., & Murray, R. M. (2006). Neurological abnormalities in schizophrenic twins. *Biological Psychiatry*, *59*, 341–348.

Power, J. D., Barnes, K. A., Snyder, A. Z., Schlaggar, B. L., & Petersen, S. E. (2012). Spurious but systematic correlations in functional connectivity MRI networks arise from subject motion (vol 59, pg 2142, 2012). *NeuroImage*, *63*, 999–999.

Rao, H., Di, X., Chan, R. C., Ding, Y., Ye, B., & Gao, D. (2008). A regulation role of the prefrontal cortex in the fist-edge-palm task: Evidence from functional connectivity analysis. *NeuroImage*, *41*, 1345–1351.

Sanders, R. D., Joo, Y. H., Almasy, L., Wood, J., Keshavan, M. S., Pogue-Geile, M. F., ... Nimgaonkar, V. L. (2006). Are neurologic examination abnormalities heritable? A preliminary study. *Schizophrenia Research*, *86*, 172–180.

Stafford, B. K., & Huberman, A. D. (2017). Signal integration in thalamus: Labeled lines go cross-eyed and blurry. *Neuron*, *93*, 717–720.

Thomann, P. A., Hirjak, D., Kubera, K. M., Stieltjes, B., & Wolf, R. C. (2015). Neural network activity and neurological soft signs in healthy adults. *Behavioural Brain Research*, *278*, 514–519.

Thomann, P. A., Wustenberg, T., Santos, V. D., Bachmann, S., Essig, M., & Schroder, J. (2009). Neurological soft signs and brain morphology in first-episode schizophrenia. *Psychological Medicine*, *39*, 371–379.

Umetsu, A., Okuda, J., Fujii, T., Tsukiura, T., Nagasaka, T., Yanagawa, I., ... Yamadori, A. (2002). Brain activation during the fist-edge-palm test: A functional MRI study. *NeuroImage*, *17*, 385–392.

van Atteveldt, N. M., Formisano, E., Goebel, R., & Blomert, L. (2007). Top-down task effects overrule automatic multisensory responses to letter-sound pairs in auditory association cortex. *NeuroImage*, *36*, 1345–1360.

Venkatasubramanian, G., Jayakumar, P. N., Gangadhar, B. N., & Keshavan, M. S. (2008). Neuroanatomical correlates of neurological soft signs in antipsychotic-naive schizophrenia. *Psychiatry Research*, *164*, 215–222.

Xu, T., Wang, Y., Li, Z., Huang, J., Lui, S. S., Tan, S. P., ... Chan, R. C. (2016). Heritability and familiality of neurological soft signs: Evidence from healthy twins, patients with schizophrenia and non-psychotic first-degree relatives. *Psychological Medicine*, *46*, 117–123.

Yazici, A. H., Demir, B., Yazici, K. M., & Gogus, A. (2002). Neurological soft signs in schizophrenic patients and their nonpsychotic siblings. *Schizophrenia Research*, *58*, 241–246.

Zhao, Q., Ma, Y. T., Lui, S. S., Liu, W. H., Xu, T., Yu, X., ... Chan, R. C. (2013). Neurological soft signs discriminate schizophrenia from major depression but not bipolar disorder. *Progress in Neuro-Psychopharmacology & Biological Psychiatry*, *43*, 72–78.

SUPPORTING INFORMATION

Additional Supporting Information may be found online in the supporting information tab for this article.

How to cite this article: Li Z, Huang J, Xu T, et al. Neural mechanism and heritability of complex motor sequence and audiovisual integration: A healthy twin study. *Hum Brain Mapp*. 2018;39:1438–1448. https://doi.org/10.1002/hbm.23935